

Data-driven simulation-based planning for electric airport shuttle systems: A real-world case study

Zhaocai Liu^a, Qichao Wang^{a,*}, Devon Sigler^b, Andrew Kotz^c, Kenneth J. Kelly^d, Monte Lunacek^e, Caleb Phillips^f, Venu Garikapati^g

^a Researcher-Computational Science, National Renewable Energy Laboratory, 15013 Denver West Parkway, Golden, CO 80401, USA

^b Researcher III-Applied Mathematics, National Renewable Energy Laboratory, 15013 Denver West Parkway, Golden, CO 80401, USA

^c Researcher III-Mechanical Engineering, National Renewable Energy Laboratory, 15013 Denver West Parkway, Golden, CO 80401, USA

^d Researcher V-Systems Engineering, National Renewable Energy Laboratory, 15013 Denver West Parkway, Golden, CO 80401, USA

^e Researcher IV-Data Science, National Renewable Energy Laboratory, 15013 Denver West Parkway, Golden, CO 80401, USA

^f Researcher V-Data Science, National Renewable Energy Laboratory, 15013 Denver West Parkway, Golden, CO 80401, USA

^g Researcher IV-Decision Support Analysis, National Renewable Energy Laboratory, 15013 Denver West Parkway, Golden, CO 80401, USA

HIGHLIGHTS

- Planning and operation of an electrified airport shuttle system.
- Event-driven simulation model is used for the evaluation of system performance.
- Data-driven simulation-based optimization for the planning of electric airport shuttle systems.
- Extensive numerical studies based on real-world operation data.

ARTICLE INFO

Keywords:

Battery electric bus
Airport shuttle system
System optimization
Simulation-based optimization

ABSTRACT

Many airports are adopting battery electric buses in their shuttle fleets due to concerns over air quality and regulations. This study proposes a simulation-based optimization modeling framework to help airport shuttle operators effectively deploy electric buses. We evaluated a planned airport electric shuttle system with an event-driven simulator. Empirical data collected from existing systems were used to drive the simulations. We then proposed a simulation-based optimization model to determine the battery capacity, charging power, and number of chargers so that predefined objective(s) (e.g., minimizing total capital cost, minimizing emissions) are optimized. Compared to existing studies, the primary contribution of the proposed method is that it can model the real-world stochastic nature of operations in an electric bus system with much higher fidelity. To demonstrate the proposed modeling framework, we study a real-world shuttle system at the Dallas-Fort Worth International Airport, and present extensive numerical studies. When considering partial fleet electrification, the model can provide a set of Pareto optimal solutions. When considering full fleet electrification, the optimal solution requires a 50-kWh battery capacity and four 210-kW chargers, resulting in a total capital cost of \$26,744,000. The results demonstrate that the proposed modeling framework can effectively optimize the planning of electric airport shuttle systems with partial or full fleet electrification.

1. Introduction

Vehicle electrification plays a key role in decarbonizing transportation systems. With the rapid development of battery [1,2], charging [3,4,5], and vehicle technologies [6,7,8,9,10], as well as

government support, the market share of electric vehicles is increasing globally. In particular, electric buses (e-buses) have enjoyed fast-growing adoption in recent years due to their potential benefits in abating local emissions, improving fuel economy, and reducing oil dependence [11,12,13]. China has led the way in adopting e-buses. With

* Corresponding author at: ESIF A308-10, 15257 Denver West Parkway, Golden, Colorado 80401, USA.

E-mail addresses: zhaocai.liu@nrel.gov (Z. Liu), qichao.wang@nrel.gov (Q. Wang).

more than 400,000 e-buses, China dominates 99 % of the e-bus market [14]. Shenzhen, a city in China, replaced all its diesel buses with 16,359 e-buses by the end of 2017 [13]. In Europe, the number of e-buses increased from around 200 to 2,200 vehicles from 2014 to 2019 [15]. Since 2016, the U.S. Federal Transit Administration (FTA) has provided a total of \$409 million to support e-bus program projects [16]. The total annual funding increased from \$55 million in 2016 to \$130 million in 2020, as shown in Fig. 1. Many bus agencies in the United States have set ambitious goals of full fleet electrification in the coming decade.

Due to the limitations of battery and charging technologies, however, e-buses have limited driving ranges and long charging times [17,18]. Compared with conventional diesel buses, which have an average range of 690 miles [19] and can easily finish a whole day's operation without refueling, e-buses usually do not have sufficient range for typical bus routes (300 to 400 miles). In addition, recharging battery e-buses usually takes much longer than refueling diesel buses. The need to evaluate the feasibility, reliability, and charging requirements of e-buses, and the absence of an effective decision support tool, bring great planning and operational challenges to transit agencies.

To design an e-bus system, bus agencies need to strategically determine the fleet size, the onboard battery capacity/driving range for the e-buses, and the needed charging infrastructure. The problem of planning e-bus systems has drawn increasing interest from researchers in recent years. Currently, there are three types of charging methods for e-buses: station-based charging, wireless lane-based charging, and battery swapping [20,21]. An et al. [22] investigated the battery-swapping facility planning problem for e-buses. The authors developed a two-stage stochastic programming model to determine the optimal deployment of battery-swapping stations and the assignment of depleted e-buses to battery-swapping stations. A real-world bus network in Melbourne, Australia, was used to verify the feasibility of the proposed model. Although battery swapping can instantly replace depleted batteries on e-buses with fully charged ones and thus produce a minimal impact on bus schedules, the high construction costs and land use requirements prohibit wide adoption of battery-swapping stations [17]. The deployment of en-route wireless lane-based charging infrastructure for e-buses has been studied by Ko and Jang [23], Jang et al. [24], Hwang et al. [25], Liu et al. [26], Liu and Song [27], and Alwesabi et al. [28]. Ko and Jang [23] and Jang et al. [24] considered only a single bus route and tried to determine the optimal location of wireless lane-based charging infrastructure and the needed onboard battery size. Hwang et al. [25] and Liu et al. [26] further studied the tradeoff between the cost of wireless charging infrastructure and the cost of onboard batteries for general bus systems with multiple routes. To hedge against charging time and energy consumption uncertainty, Liu and Song [27] developed a robust optimization model for the planning of wireless charging e-bus systems.

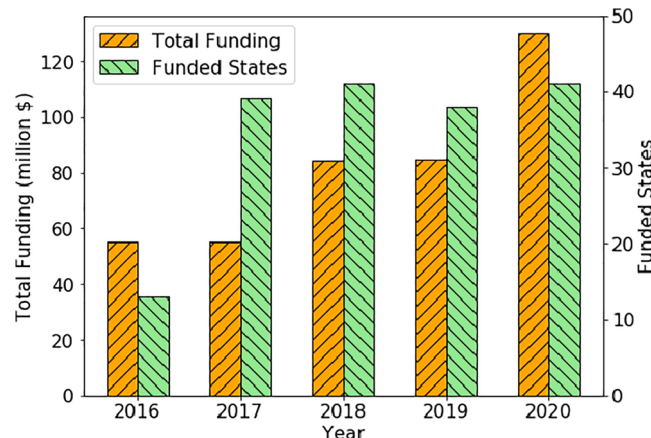


Fig. 1. The total funding and number of funded states from the U.S. FTA for e-bus projects.

Alwesabi et al. [28] extended this work by considering e-bus fleet sizing. The above studies focus on minimizing the total system monetary cost. Bi et al. [29] addressed wireless charger deployment for an e-bus network using a multi-objective life cycle optimization approach, which considers the economic, environmental, and energy burdens. Bi et al. [30] compared life cycle energy and greenhouse gas emissions of wireless vs plug-in charging for an e-bus system, and found that the wireless charging system consumed 0.3 % less energy and emitted 0.5 % less greenhouse gases than plug-in charging over the total life cycle in the base case analysis. For a comprehensive review of en-route wireless charging technology and its application in e-bus systems, readers are referred to Bi et al. [31] and Jang [32]. Although wireless lane-based charging provides a flexible in-motion charging capability, it has not been widely applied to e-bus systems due to the high construction costs associated with installing wireless charging facilities underneath roadways [17]. Currently, station-based charging is the most widely used charging method for e-buses. Electric vehicle chargers can be divided into level 1, level 2, and level 3 based on their charging powers. Table 1 shows the characteristics of the three different power levels [33]. Level 1 and level 2 chargers are usually alternating current (AC) chargers that directly connect the electrical grid to an electric vehicle's onboard charger; the onboard charger then converts the received AC into direct current (DC) for the battery. Level 3 chargers are usually DC chargers that directly convert AC to DC, then "bypass" an electric vehicle's onboard charger and send the DC to the battery. For e-buses, AC slow chargers can be used at bus depots for overnight charging, and DC fast chargers can be installed at terminals or bus stops, enabling opportunity charging. Kunith et al. [11] proposed a mixed-integer linear program to optimize the deployment of charging stations and the onboard battery sizes of e-buses. Liu et al. [18] extended this work by developing a robust optimization model to consider the uncertainty of bus energy consumption. An [17] developed a stochastic integer program to optimize charging facility location and fleet size for e-bus systems considering stochastic charging demand. In contrast to Kunith et al. [11] and Liu et al. [18], who considered installing fast charging stations at candidate bus stops and terminals, An [17] focused on deploying regular charging stations at bus terminals or depots. Rogge et al. [34] addressed the e-bus depot charger deployment problem considering the scheduling of battery e-buses and the fleet composition.

In this paper, we focus on the planning problem of e-bus systems within an airport. Airport bus systems play a key role in the safe and efficient transportation of passengers, flight personnel, and airport employees. Motivated by concerns about air quality impacts and regulations, many airports are transitioning vehicles and equipment to technologies that reduce emissions, such as battery electric vehicles [35]. For instance, California has required thirteen state airports to exclusively operate zero-emission vehicles by December 31, 2035. However, studies addressing the planning problem of electric airport bus systems are sparse. To the best of our knowledge, Helber et al. [12] is the only relevant study. Helber et al. [12] developed a binary linear program to optimize the deployment of wireless lane-based charging infrastructure for electric airport buses. The proposed model minimizes the total capital cost of the charging infrastructure while ensuring that, for each bus service trip, the amount of energy charged to the e-bus is enough to serve the trip. Numerical experiments based on a small fictitious airport bus network were conducted to demonstrate the

Table 1
Charging Power Levels.

Power Level	Charger Location	Typical Use	Typical Power	Charging Time
1	On board	Home	2 kW	4–11 h
2	On board	Public	20 kW	1–4 h
3	Off board	DC fast	100 kW	less than 30 min

effectiveness of the proposed model. In contrast to Helber et al. [12], the current paper considers station-based charging because it is currently the most widely used charging method for e-buses. Compared to wireless lane-based charging, the key challenge for modeling station-based charging systems is the need to consider the charging capacity and detailed queuing behavior of e-buses at charging stations. Note that there is no fundamental difference between planning airport e-bus systems and other e-bus systems in the existing research. Therefore, existing planning methods for e-bus systems proposed in the literature might also be applicable to airport e-bus systems. However, existing studies usually optimize e-bus system design using pure mathematical programs, which tend to simplify the operation of an e-bus system for model tractability. For instance, existing studies typically neglect bus capacity, passenger queuing behavior at bus stops, and e-bus queuing behavior at charging stations. Compared to city bus systems, airport shuttle systems usually have a much simpler structure and passenger demands, which makes it possible to use high-fidelity simulation to model airport shuttle systems.

This paper develops a simulation-based optimization framework to address the planning problem of electric airport bus systems. The modeling framework has a two-level structure. In the lower level, we use an event-driven simulation model, Airport Shuttle Planning and Improved Routing Event-driven Simulation (ASPIRES), which was developed by our research team [36,37], to evaluate the expected performance of a designed electric airport shuttle system using detailed day-to-day operations under stochastic traffic conditions, passenger demand, and vehicle energy consumption. In the upper level, we optimize the design of the electric airport shuttle system based on certain predefined objectives. The modeling framework can consider different design variables, including onboard battery size, number of chargers, and charging power for chargers. It can consider both full fleet electrification and partial fleet electrification.

The primary contribution of the present study is threefold. First, this work informs the development of e-bus charging features in ASPIRES for the charging station planning problem for an electric airport bus system. Second, compared to the aforementioned studies, which optimize e-bus system design using pure mathematical programs, the proposed simulation-based optimization framework can model the real-world stochastic nature of e-bus system operations with much higher fidelity. For instance, the simulation model can explicitly consider the vehicle capacity, stochastic passenger arrival, stochastic energy consumption, and stochastic travel time of e-buses, as well as the charging capacity and detailed queuing behavior at bus stops and charging stations. It is challenging to consider all those features with high fidelity in pure mathematical programs while ensuring the computational tractability. Third, this study applies the proposed modeling framework to a real-world airport shuttle bus system at Dallas-Fort Worth International Airport (DFW). We utilize real-world operation data from the shuttle system that connects the five terminals and the rental car center at DFW. Based on the real-world data, we conduct extensive numerical studies to demonstrate the effectiveness of the proposed modeling framework.

The remainder of this paper is structured as follows. Section 2 defines the charging station planning problem for an electric airport shuttle bus system. Section 3 presents a simulation-based optimization modeling framework to address the planning problem. To make this paper self-contained, we also present descriptions of the ASPIRES simulation model. Numerical studies based on real-world operation data from the DFW airport bus system are provided in Section 4. Finally, in Section 5, conclusions from this work are drawn.

2. Problem description

Services provided by bus systems within an airport include airside transfer, terminal transfer, car parking transfer, and rental car center transfer. The bus system at DFW that connects the five terminals (Terminals A, B, C, D, and E) and the rental car center is used as an example

to define the charging station planning problem. Fig. 2 shows the configuration of the five terminals at DFW. The rental car center is located about 2.5 miles south of Terminal E. A fleet of 46 buses is used to transport passengers between the five terminals and the rental car center. Service trips include R-A-R, R-B-R, R-C-R, R-D-R, R-E-R, R-A-B-R, R-B-A-R, and R-C-D-R, where R represents the rental car center and A, B, C, D, and E represent the respective terminals. Terminals A–D each have two bus stops, while Terminal E has three stops. The rental car center has a drop-off location and five pickup locations corresponding to the five terminals. Assuming operators of the bus system plan to convert the fleet into battery e-buses, the problem to solve is determining the installation of charging stations, their charging power, and the capacity of the on-board bus batteries. The performance of the designed e-bus system can be evaluated using different criteria, including the total capital investment, the average passenger waiting time, and (when the fleet is only partially electrified) the total miles traveled by nonelectric vehicles. Although the airport bus system only has seven types of trips and seventeen bus stops, it is nontrivial to model the system and evaluate its operation. First, the airport bus system has no predefined timetable. It only has a rough service target for headway (the time between bus arrivals at stops), and it might modify its service based on real-time passenger demand. Second, the travel time and energy consumption of buses are uncertain due to the highly stochastic traffic conditions and passenger demand at the airport. Third, without a timetable and with highly stochastic charging demand, it is difficult to model the queuing process at charging stations.

Major assumptions included in the model are listed below. Note that the problem identified in this paper is part of an ongoing collaboration between NREL and DFW. These assumptions have been chosen based on meetings and conversations with the bus operation staff at DFW.

- (1) The electric airport shuttle system will operate according to the previously established service frequency requirements.

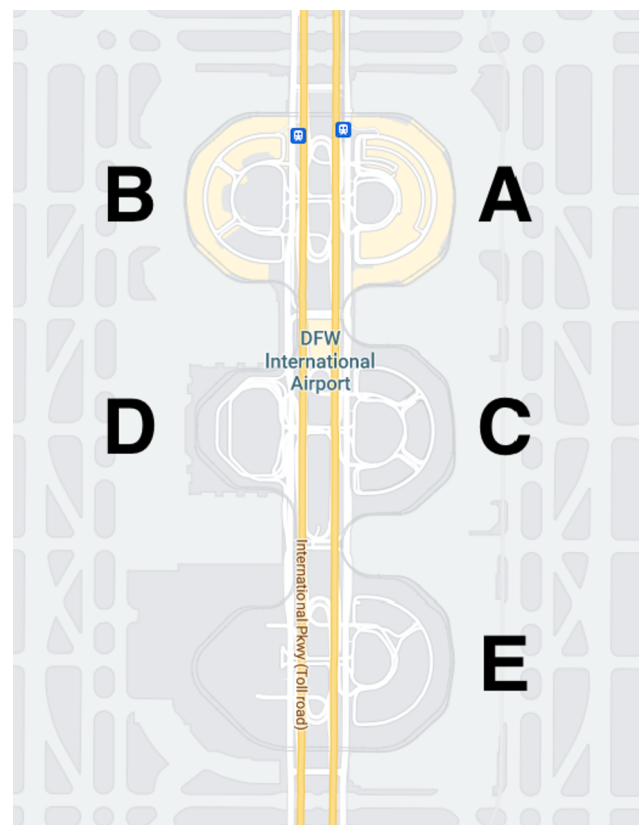


Fig. 2. The layout of the DFW airport.

- (2) All the e-buses are homogeneous and have the same driving range.
- (3) The energy recharged is the product of charging power, charging efficiency, and charging duration.
- (4) The chargers installed at the charging station are homogeneous, and each charger has one outlet.

3. Simulation-Based optimization

In this section, we first introduce ASPIRES, the event-driven simulation model developed by our research team at NREL (see [36] for the source code). Based on the simulation model, we then propose a simulation-based optimization model to address the strategic planning problem for an electric airport shuttle bus system. As mentioned in the introduction, the modeling framework has a two-level structure. Fig. 3 shows a schematic of the two-level structure. In the lower level, we use ASPIRES to simulate the detailed day-to-day operations of a designed electric airport shuttle system under stochastic traffic conditions, passenger demand, and vehicle energy consumption and evaluate the expected performance of the system. In the upper level, we optimize the shuttle system based on certain predefined objectives concerning costs and emissions.

3.1. ASPIRES simulation model

Most traffic simulation packages have hard-to-calibrate problems. The ASPIRES simulation model tries to address this issue. ASPIRES is mainly driven by empirical distributions of real-world data. Instead of calibrating the simulation, we use the data to drive the simulation. With more data, the simulation will be more realistic. The ASPIRES simulation model provides fast simulations of the airport shuttle service. It has been optimized for runtime speed; simulating one day of shuttle operations takes around one second. The ability to execute fast simulations enables the exploration of many different infrastructure configurations and operational policies under a wide range of different scenarios.

ASPIRES can simulate travel times, dwell times, and passenger arrivals using empirical distributions derived from real data that capture the stochastic nature of DFW's rental car center shuttle bus operations. Additionally, ASPIRES can collect relevant data that can be used for system analysis. The simulation outputs show passenger statistics, shuttle statistics, and charging station statistics. The passenger statistics include the waiting time of each passenger, the queue length of each stop at any time, the total travel time from one stop to another, and the number passengers left after each shuttle bus pickup. The shuttle statistics include a record of routes driven, the number of passengers onboard at any time, the distance traveled up until any time, the energy consumed until any time, and the location of each bus at any time. The charging station statistics record the number of chargers being used at any time of the day. ASPIRES has been adopted by Sigler et al. [38] in route optimization for energy efficient airport shuttle operations.

ASPIRES was developed using SimPy, a discrete event simulation package for Python [39]. ASPIRES uses three sets of SimPy resources, one for the buses, one for the stops, and one for the charging stations. The passengers arrive at the stops following time-dependent Poisson

processes; the passengers' mean arrival times are derived from real-world data. The shuttle buses move along the routes they serve. At each stop, a shuttle drops off some passengers and picks up others until all the passengers have been picked up or the bus becomes full. In a given day, different numbers of buses are needed at different times, and the bus routes may vary (e.g., at night, before returning back to the rental car center, a bus may serve two terminals, whereas daytime buses might serve only one terminal in a route). Because of this, the simulation has a dispatcher who manages the number of buses on different routes. Below, we discuss the development of the event-based simulation model.

3.1.1. Stop-Based vehicle and passenger movement

An airport bus system can be represented abstractly as a directed graph $G(N, A)$, where the node set N represents the set of bus stops, and the arc set A represents the set of links connecting two bus stops. Let M represent the set of all buses. For each bus $m \in M$, let L_m denote the set of trips or routes executed by the bus within a certain period of observation. For the bus system connecting the five terminals and the rental car center at DFW, each trip is defined as a journey from the rental car center to one or two terminals and back to the rental car center. For each trip $l \in L_m$, let N_l and A_l denote the set of nodes and arcs along the trip, respectively.

For each bus stop $n \in N$, a variable $\alpha_n(t)$ is used to track the total accumulative number of passengers waiting at the stop until time t . Note that $t = 0$ denotes the simulation starting time. As mentioned previously, passenger arrival at a bus stop is modeled as a Poisson process. The headway between two passenger arrival events at a stop can thus be specified by an exponential distribution [40]. Suppose a passenger arrives at a bus stop $n \in N$ at time t_0 and the passenger arrival rate is denoted by $\lambda(t_0)$. The time interval for the next passenger arrival can be calculated as $\frac{-1}{\lambda(t_0)} \ln r$, where r is a uniformly distributed random number on $(0, 1)$. We can thus compute the time t when the next passenger arrives and calculate the next $\alpha_n(t)$ as follows:

$$\alpha_n\left(t_0 + \frac{-1}{\lambda(t_0)} \ln r\right) = \alpha_n(t_0) + 1 \quad \forall n \in N \quad (1)$$

For each bus stop $n \in N$, another variable $\beta_n(t)$ is introduced to track the total accumulative number of passengers picked up at the stop until time t . When a bus arrives at a stop, it first drops off the passengers whose destination is the stop and then picks up the passengers waiting at the stop. The total number of onboard passengers should not exceed the bus capacity. With $\alpha_n(t)$ and $\beta_n(t)$ respectively tracking the passenger arrival and passenger departure at a bus stop $n \in N$, the waiting time of each passenger can be calculated, assuming people get on buses in the order they arrive at the bus stop.

For each trip $l \in L_m$ served by a bus $m \in M$, let $\tau_{a,l,m}$ and $e_{a,l,m}$ respectively denote the travel time and energy consumption on each arc $a \in A_l$, and let $\tau_{n,l,m}$ and $e_{n,l,m}$ respectively denote the dwell time and energy consumption at each stop $n \in N_l$. Data describing $\tau_{a,l,m}$, $e_{a,l,m}$, $\tau_{n,l,m}$, and $e_{n,l,m}$ can be collected from real-world operations. If variables $t_{n,l,m}^{arr}$ and $t_{n,l,m}^{dep}$ are introduced to track the time when a bus m arrives at and departs from stop n of trip l , we have:

$$t_{n,l,m}^{dep} = t_{n,l,m}^{arr} + \tau_{n,l,m} \quad \forall m \in M, l \in L_m, n \in N_l \quad (2)$$

If n_a^+ and n_a^- represent the head and tail nodes of arc a , respectively, we also have:

$$t_{n_a^+, l, m}^{arr} = t_{n_a^-, l, m}^{dep} + \tau_{a, l, m} \quad \forall m \in M, l \in L_m, a \in A_l \quad (3)$$

Let $\gamma_{n,l,m}^{off}$ and $\gamma_{n,l,m}^{on}$ denote the number of passengers getting off and on the bus at each stop $n \in N_l$. If $h_{n,l,m}^{arr}$ and $h_{n,l,m}^{dep}$ denote the number of onboard passengers when a bus m arrives at and departs from stop n on trip l , we have:

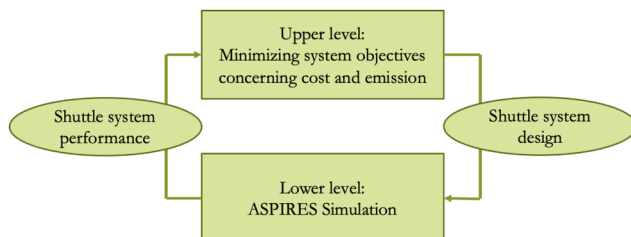


Fig. 3. The two-level structure of the simulation-based optimization.

$$h_{n,l,m}^{dep} = h_{n,l,m}^{arr} - \gamma_{n,l,m}^{off} + \gamma_{n,l,m}^{on} \quad \forall m \in M, l \in L_m, n \in N_l \quad (4)$$

$$\gamma_{n,l,m}^{on} = \min \left\{ h_{n,l,m}^{max} - (h_{n,l,m}^{arr} - \gamma_{n,l,m}^{off}), \alpha_n(t_{n,l,m}^{dep}) - \beta_n(t_{n,l,m}^{arr}) \right\} \quad \forall m \in M, l \in L_m, n \in N_l \quad (5)$$

$$\beta_n(t_{n,l,m}^{dep}) = \beta_n(t_{n,l,m}^{arr}) + \gamma_{n,l,m}^{on} \quad \forall m \in M, l \in L_m, n \in N_l \quad (6)$$

where h^{max} represents the maximum capacity of a bus. The remaining space of vehicle m is given by $h^{max} - (h_{n,l,m}^{arr} - \gamma_{n,l,m}^{off})$, and the number of passengers waiting at the stop is given by $\alpha_n(t_{n,l,m}^{dep}) - \beta_n(t_{n,l,m}^{arr})$.

3.1.2. Development of electric bus charging features

Let e^{max} denote the battery capacity of an e-bus. If variables $s_{n,l,m}^{arr}$ and $s_{n,l,m}^{dep}$ are introduced to track the battery state of charge (SoC) (a value between 0 and 1) for e-bus m when it arrives at and departs from stop n when serving trip l , we have:

$$e^{max}s_{n,l,m}^{dep} = e^{max}s_{n,l,m}^{arr} - e_{n,l,m} \quad \forall m \in M, l \in L_m, n \in N_l \quad (7)$$

$$e^{max}s_{n_a,l,m}^{arr} = e^{max}s_{n_a,l,m}^{dep} - e_{n_a,l,m} \quad \forall m \in M, l \in L_m, a \in A_l. \quad (8)$$

For the bus system connecting the five terminals and the rental car center at DFW, the charging station can be installed at the rental car center or other predetermined locations near the rental car center (e.g., the bus depot, or the existing bus refueling station). When an e-bus returns to the rental car center after finishing a service loop, its battery SoC will be checked. If the expected battery SoC of an e-bus after its next trip will fall below a prespecified lower bound, the e-bus will go to the charging station to get charged. When the number of e-buses is greater than the number of chargers installed at the charging station, charging queues might form at the charging station. Charging services are assumed to follow the first-come, first-served rule. The chargers at the charging station are modeled as resources that can be used by a limited number of e-buses. The total number of occupied and available chargers at the charging station is tracked over time. Let d denote the graph node that represents the charging station. Let σ and δ denote the charging power and charging efficiency of the chargers, respectively. Let $s_{d,l,m}^{arr}$ and $t_{d,l,m}^{arr}$ represent the battery SoC and time when bus m arrives at the charging station after finishing trip l , respectively. Let $\tau_{d,l,m}^{waiting}$ and $\tau_{d,l,m}^{charging}$ be the waiting time before getting an available charger and the charging time, respectively. Let $s_{d,l,m}^{dep}$ and $t_{d,l,m}^{dep}$ denote the battery SoC and the time when the bus leaves the charging station, respectively. Finally, let s^{up} denote the safety upper bound for battery SoC. We then have the following relationships:

$$s_{d,l,m}^{dep} = s^{up} \quad \forall m \in M, l \in L_m \quad (9)$$

$$\tau_{d,l,m}^{charging} = \frac{e^{max}(s_{d,l,m}^{dep} - s_{d,l,m}^{arr})}{\sigma\delta} \quad \forall m \in M, l \in L_m \quad (10)$$

$$t_{d,l,m}^{dep} = t_{d,l,m}^{arr} + \tau_{d,l,m}^{waiting} + \tau_{d,l,m}^{charging} \quad \forall m \in M, l \in L_m. \quad (11)$$

To model the bus to service trip assignment, we divide each day into 24 h and collect the service frequency for each type of trip. Based on the service frequency and the time needed to finish each type of trip, the number of vehicles needed to serve each type of trip within each hour can be estimated, and then buses can be assigned to each type of trip accordingly. Due to changes in service frequency, a bus might switch from one type of trip to another or go idle.

To summarize, we modeled the following events for the operation of an airport bus system: (1) passengers accumulate at bus stops, (2) a bus starts a new service trip after finishing the last trip, (3) a bus moves from

one stop to the next stop, (4) a bus drops off and picks up passengers at a stop, (5) an e-bus drives to a charging station, (6) an e-bus waits for an available charging station, (7) an e-bus finishes charging at a charging station, (8) a bus is idling and waiting for the next trip request, (9) a charger at the bus depot is occupied, and (10) a charger at the bus depot is released and becomes available. Key status variables of an airport bus system are tracked and updated using Eqs. (1)–(11). In the ASPIRES simulation model, parameters about travel times, dwell times, passenger arrivals, and vehicle energy consumption are randomly drawn from empirical distributions derived from real-world data. The simulation model can provide stochastic results for each run, which captures the stochastic nature of the shuttle system operation in the airport area.

3.2. Simulation-Based optimization model

Using the ASPIRES model to evaluate the performance of a designed electric airport bus system, we further develop a simulation-based optimization model to address the charging station planning problem for the bus system. Let x denote the number of chargers to be installed. The strategic planning problem for the electric airport shuttle bus system can be formulated as the following optimization problem:

$$\min_{x, \sigma, e^{max}} f(x, \sigma, e^{max})$$

subject to

$$x \in \{1, 2, \dots, |M|\} \quad (12)$$

$$\sigma \in \{\sigma_1, \sigma_2, \dots, \sigma_{k_1}\} \quad (13)$$

$$e^{max} \in \{e_1^{max}, e_2^{max}, \dots, e_{k_2}^{max}\} \quad (14)$$

$$\phi(x, \sigma, e^{max}) \geq 0, \quad (15)$$

where $\{\sigma_1, \sigma_2, \dots, \sigma_{k_1}\}$ represent k_1 different candidate levels of charging power for the e-bus chargers, $\{e_1^{max}, e_2^{max}, \dots, e_{k_2}^{max}\}$ represent k_2 different bus battery capacities, and functions $f(x, \sigma, e^{max})$ and $\phi(x, \sigma, e^{max})$ are evaluated using the simulation model. Constraints (12)–(14) specify the possible values of x , σ , and e^{max} , respectively. Constraint (15) defines a set of constraints to be specified by decision-makers. Objective function $f(x, \sigma, e^{max})$ can be a single scalar objective or a vector of two or more objectives.

When the bus fleet is partially electrified, we aim to minimize miles traveled by nonelectric buses and the total capital cost while ensuring constraints that specify an acceptable level of service are met. Specifically, the objective function.

$\min_{x, \sigma, e^{max}} f(x, \sigma, e^{max})$ and constraint $\phi(x, \sigma, e^{max}) \geq 0$ are defined as follows:

$$\min_{x, \sigma, e^{max}} f(x, \sigma, e^{max}) = \min_{x, \sigma, e^{max}} \left\{ x^* P^{charger}(\sigma) + P^{BEB}(e^{max}) * N^{BEB} \sum_{n \in \{1, 2, \dots, N^{Other}\}} Q^n(x, \sigma, e^{max}) \right\}$$

$$\phi(x, \sigma, e^{max}) = W^{max} - W(x, \sigma, e^{max}) \geq 0,$$

where $P^{charger}(\sigma)$ is the price of a charger with charging power σ , $P^{BEB}(e^{max})$ is the cost of an e-bus with battery capacity e^{max} , N^{BEB} is the number of e-buses, N^{Other} is the number of nonelectric buses, $Q^n(x, \sigma, e^{max})$ is the total miles traveled by nonelectric bus $n \in \{1, 2, \dots, N^{Other}\}$, W^{max} is the maximum allowable passenger mean waiting time, and $W(x, \sigma, e^{max})$ is the passenger waiting time with design (x, σ, e^{max}) . Note that $Q^n(x, \sigma, e^{max})$ and $W(x, \sigma, e^{max})$ will be collected from the simulation. Further, $x^* P^{charger}(\sigma) + P^{BEB}(e^{max}) * N^{BEB}$ defines the total capital cost of chargers and e-buses, $\sum_{n \in \{1, 2, \dots, N^{Other}\}} Q^n(x, \sigma, e^{max})$ is the total miles traveled by nonelectric buses, and constraint $W^{max} - W(x, \sigma, e^{max}) \geq 0$ ensures that the passenger mean waiting time is smaller than the

allowed value.

When the whole bus fleet is electrified, we minimize a single objective—total capital cost—while ensuring acceptable passenger waiting time. Specifically, the objective function.

$\min_{x, \sigma, e^{max}} f(x, \sigma, e^{max})$ and constraint $\phi(x, \sigma, e^{max}) \geq 0$ are defined as follows:

$$\min_{x, \sigma, e^{max}} f(x, \sigma, e^{max}) = \min_{x, \sigma, e^{max}} x^* P^{charger}(\sigma) + P^{BEB}(e^{max}) * N^{BEB}$$

$$\phi(x, \sigma, e^{max}) = W^{max} - W(x, \sigma, e^{max}) \geq 0$$

Although we consider the fleet size to be a given parameter in this paper, for our simulation-based optimization framework, the number of e-buses can be another system design variable, denoted by $y \in \{N^{min}, N^{min}+1, N^{min}+2, \dots, N^{max}\}$, where N^{min} and N^{max} are the minimal and maximal fleet sizes, respectively. Then, the domain for the number of chargers can be updated to $x \in \{1, 2, \dots, y\}$, and the decision variable vector will become (y, x, σ, e^{max}) . We can use the simulation to evaluate the performance of each bus system design $(y, x, \sigma, e^{max})^*$ during operation, and we can use the simulation-based optimization method to optimize the system design, including the number of e-buses.

The above problem is a two-level problem. The lower level is a simulation model used to evaluate the expected performance of a designed electric airport shuttle system using detailed day-to-day operations under stochastic traffic conditions, passenger demand, and vehicle energy consumption. The upper-level problem must decide the values for charging station deployment ($x \in \{1, 2, \dots, |M|\}$) and $\sigma \in \{\sigma_1, \sigma_2, \dots, \sigma_{k_1}\}$) and the battery capacity for the fleet's e-buses ($e^{max} \in \{e_1^{max}, e_2^{max}, \dots, e_{k_2}^{max}\}$). A brute force enumeration can be used to solve the problem when the total number of potential solutions (i.e., $|M| \times k_1 \times k_2$) can be evaluated using the simulation model within an acceptable amount of time. Although brute force enumeration can ensure a global optimal solution, this approach is not always possible when a large decision space is being considered. This paper develops a genetic-algorithm-based solution procedure (see Fig. 4) to solve the problem when the decision space is too large for complete enumeration. The solution procedure includes two main modules: a simulation module and a genetic algorithm module. The simulation module evaluates the performance of each solution. The genetic algorithm module is used to find near-optimum solutions.

Essentially, the genetic-algorithm-based approach encodes the decision variables of the upper-level problem (i.e., the values for charging station deployment and the battery capacity) into a number of chromosomes (i.e., strings). Then, the fitness value of each chromosome is calculated using the simulation model. Because selection, reproduction, crossover, and mutation operations are conducted iteratively from the genetic algorithm, selective pressure drives the population to more

effective regions of the search space. After a given number of iterations, the genetic algorithm terminates and returns the best identified solutions.

1) **Initialization:** Randomly generate pop_size chromosomes, where pop_size denotes the population size. Each chromosome $C = (c_1, c_2, c_3)$ represents a solution (x, σ, e^{max}) , where c_i represents the i th decision variable.

2) **Evaluation Function:** Each chromosome's likelihood of reproduction is measured using an evaluation function. The negative of the objective function minus a penalty term is used as the evaluation function, i.e., $Eval(C) = -f(x, \sigma, e^{max}) - G\phi(x, \sigma, e^{max})$, where $Eval(C)$ represents the evaluation function and G is a large enough constant to penalize the inequality constraint $\phi(x, \sigma, e^{max}) \geq 0$. Note that the best solution has the maximal value of $Eval(C)$.

3) **Selection Process:** The roulette wheel selection method is used to select the next generation of chromosomes. Based on the evaluation function values, we order the chromosomes and define $p_0 = 0$, $p_i = \sum_{j=1}^i Eval(C_j)$, and $i = 1, 2, \dots, pop_size$. Then, we can select a chromosome by first randomly generating a number $\varpi \in (0, p_{pop_size}]$ and then selecting the chromosome C_i such that $\varpi \in (p_{i-1}, p_i]$.

4) **Crossover Operation:** Let $Prob_co$ denote the crossover probability. We first randomly generate a real number $\varpi \in [0, 1]$ and pick two parent chromosomes C_i and C_j . If $\varpi < Prob_co$, we produce two new chromosomes using C_i and C_j via the crossover operator. Because each chromosome has three variables, we randomly switch one variable value from the two parent chromosomes. For instance, if $C_i = (c_1, c_2, c_3)$ and $C_j = (\hat{c}_1, \hat{c}_2, \hat{c}_3)$, two new chromosomes $C^{Child1} = (c_1, \hat{c}_2, \hat{c}_3)$ and $C^{Child2} = (c_1, \hat{c}_2, \hat{c}_3)$ can be created.

5) **Mutation Operation:** Let $Prob_mt$ denote the mutation probability. We first randomly generate a real number $\varpi \in [0, 1]$ and pick one chromosome C_i . If $\varpi < Prob_mt$, we randomly select a variable of the chromosome and replace it with a randomly generated new variable value.

The aforementioned process is outlined below. Note that pop_size and $max_generation$ can be chosen based on available computing resources and time. For the choice of $Prob_co$ and $Prob_mt$, readers are referred to the review paper by Patil and Pawar [41] for relevant discussions.

Step 0: Define the fitness function and specify the following parameters for the genetic algorithm: population size pop_size , maximum number of generations $max_generation$, crossover probability $Prob_co$, and mutation probability $Prob_mt$.

Step 1: Initialize the population by randomly generating pop_size chromosomes and set the generation index to $g = 1$.

Step 2: Run the simulation model for each chromosome and calculate the fitness accordingly. Reproduce the population based on the distribution of fitness values.

Step 3: Conduct the crossover and mutation operations.

Step 4: If $g = max_generation$, terminate and obtain the optimal solution(s). Else, set $g = g + 1$ and go to Step 2.

4. Numerical studies

To test the proposed simulation-based design framework, we carry out numerical studies based on the real-world airport bus system that connects the five terminals and the rental car center at DFW. We first present and discuss the real-world operation data from DFW that was used. Then, in Section 4.2, we demonstrate the simulation model using a predetermined system design. Section 4.2 shows some key outputs that can be extracted from the simulation model, including total miles traveled by e-buses and compressed natural gas (CNG) buses, SoC profile of each e-bus, charger usage profile, and passenger waiting time. Section 4.2 also shows the potential impact of battery size, charging power, and number of chargers on the total miles traveled by CNG buses for the scenario with 10 e-buses. Section 4.2 demonstrates how the lower-level

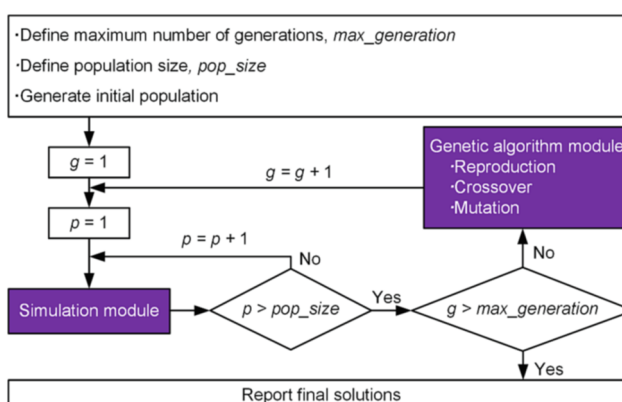


Fig. 4. Procedure for the genetic-algorithm-based approach.

simulation model can be used to simulate the detailed day-to-day operations of a designed electric airport shuttle system under stochastic traffic conditions, passenger demand, and vehicle energy consumption, and to evaluate the expected performance of the system. Lastly, in Section 4.3, we demonstrate how the two-level simulation-based optimization model can be used to optimize the system design.

Note that the problem identified in this paper is part of an ongoing collaboration between NREL and DFW. The assumptions and numerical study scenarios used here were chosen based on meetings and conversations with the bus operation staff at DFW.

4.1. Data description

This study primarily uses two sets of data. First, in collaboration with DFW, NREL researchers use vehicle data loggers to collect controller area network (CAN) bus data from the airport shuttles [42]. The data provides information on vehicle position, speed, fuel rate, engine power output, and other vehicle parameters at a 1 Hz frequency, giving a second-by-second snapshot of the energy consumption and operational state of the vehicle. Second, Spatial Positioning on Transit (SPOT) data is collected by DFW. SPOT is ETA Transit System's computer-aided dispatch/automatic vehicle location (CAD/AVL) system. It collects and reports detailed bus operation data that can be used to analyze bus ridership changes, public site usage, passenger demands at each stop, whether buses are operating on time, whether vehicles are running routes as prescribed, etc.

The CAN data includes second-by-second geolocation information for each monitored bus, from which we can extract the dwell time at each stop as well as the distance and travel time of each trip segment. CAN data also includes detailed fuel consumption information for each trip segment. For instance, Fig. 5(a) shows the distribution of bus travel time, and Fig. 5(b) shows the distribution of bus energy consumption for the trip segment from the rental car center to Terminal E. Considering the time-varying passenger demand and traffic conditions, we group CAN data points based on the time of day and the day of the week. For each day of the week, we divide the 24 h into six equal-length intervals and group the data points together for each interval.

SPOT data provides detailed information about the time of events, stop locations, boarding and alighting, and the trip type for each bus. In this study, we collected SPOT data from December 1, 2019, to February 17, 2020. We extracted fleet size, service frequency, and passenger boarding and alighting data at each stop from the SPOT data. Fig. 6 shows the hourly number of shuttle visits for each terminal over one representative day. One can observe from Fig. 6 that the bus service frequency varies significantly over the day; this is due to the time-varying flight traffic and the resulting passenger demand. Therefore, we extracted the average service frequency for each hour in each day of the week. Similarly, passenger boarding and alighting for each bus stop

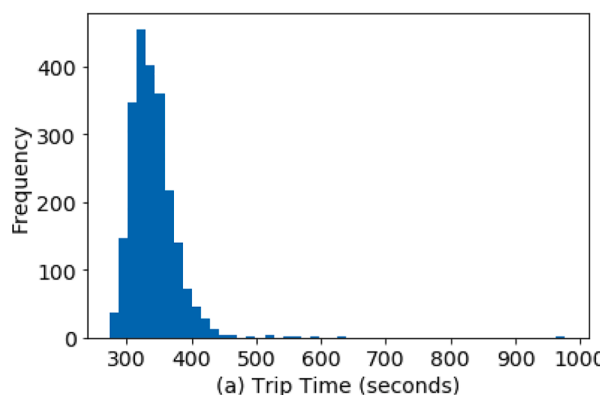


Fig. 5. Empirical distribution of (a) bus travel time and (b) bus energy consumption for the trip segment from the rental car center to Terminal E.

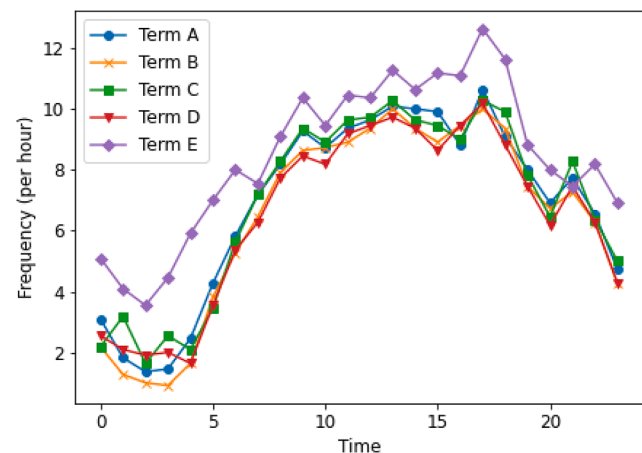


Fig. 6. Hourly number of shuttle visits for each terminal over the course of a day.

can also be extracted from the SPOT data. For instance, Fig. 7 shows the average boarding data for the first stop in Terminal E on Monday.

4.2. Simulation experiments

Currently, the shuttle system connecting the five terminals and the rental car center at DFW runs on compressed natural gas (CNG). If we assume that DFW plans to convert 10 CNG buses into battery e-buses,

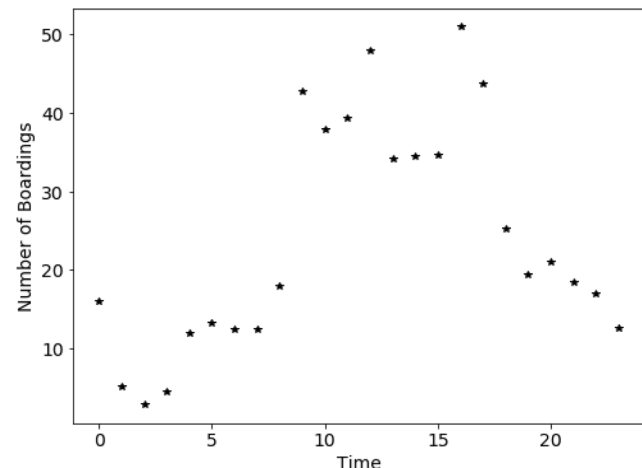
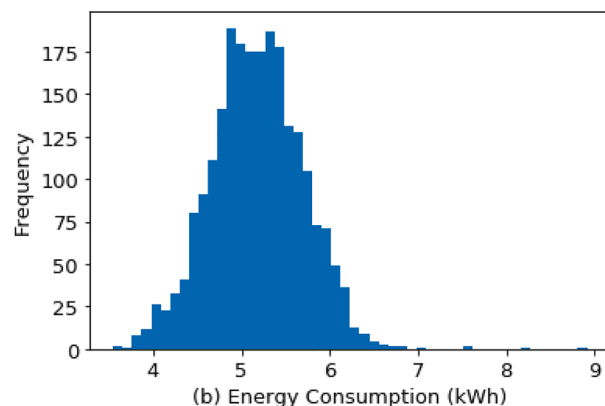


Fig. 7. Boarding data for the first stop in Terminal E on Monday.



then using the proposed simulation model, we can evaluate the performance of the new mixed-fleet bus system. Further, let us assume the 10 battery e-buses have a battery capacity of 100 kWh, with upper and lower SoC bounds being 85 % and 20 %. Suppose 10 chargers with a charging power of 100 kW and a charging efficiency of 91.4 % [43] will be installed at a charging station that is 2.5 miles away from the rental car center. We simulated the operations of this bus system for 29 days, with the first day being a warm-up day for the simulation. Using a 2.4-GHz Mac computer with 16 GB of RAM, it took 125.1 s to run the simulation.

Over the 28-day operation period, 392,681 passengers were served by the shuttle bus system. The mean waiting time for those passengers was 343.1 s. The whole bus fleet traveled 214,822.8 total miles, with 166,432.1 miles from CNG buses and 48,390.7 miles from e-buses. Fig. 8 shows a sample SoC profile of an e-bus during the first week of the simulation (with the warm-up day excluded). Throughout the five days, the SoC of the e-bus was roughly within the specified range (i.e., 20 % to 85 %). Due to stochastic energy consumption, the 20 % battery SoC lower bound was violated once between hours 100 and 125. This result demonstrates the necessity of a safe battery SoC lower bound. Fig. 9 shows the charger usage profiles for the 28 days and for the first day. The maximum number of chargers in use throughout the 28 days was five, which implies that we might be able to remove five chargers without impacting the operation of the 10 e-buses.

The bus system under the status quo scenario, i.e., with no e-buses, was also simulated. Fig. 10 compares the passenger waiting time distribution between the status quo scenario and the scenario with 10 e-buses. One can observe that the 10 deployed e-buses have a negligible impact on passenger waiting times. This result is expected because the studied bus system has a fleet size of 46, but only 29 buses are needed to ensure the maximum service frequency found in the SPOT data. Even when all 10 e-buses need to go charge, the bus system still has enough buses to ensure normal operations.

An e-bus with a small battery capacity will frequently need to use the charging station and thus might waste a lot of time traveling to and from the charging station. To test the impact of battery capacity on the performance of the bus system, we ran the simulation model with the battery capacity ranging from 50 kWh to 300 kWh, with a step size of 50 kWh. The average daily miles traveled by CNG buses are used to measure the performance of the bus system. They can be considered a gross indicator of greenhouse gas emissions. Fig. 11 shows the average daily miles traveled by CNG buses in the fleet with different battery capacities for the e-buses. For the most part, the average daily miles traveled by CNG buses decreases as battery capacity for the e-buses increases. This

result is expected because with larger battery capacities, e-buses require fewer charging events during operation and waste less time traveling to and from the charging station; consequently, they can replace more miles traveled by CNG buses. Note that the average daily miles traveled by CNG buses increases slightly when the battery capacity increases from 200 kWh to 250 kWh; this is likely due to the stochasticity of the simulation.

When charging power is low, e-buses need to spend a long time charging and thus have a low service time. Moreover, when the number of chargers is limited and the charging power is low, a charging queue might form at the charging station. To test the impact of the number of chargers and the charging power, we ran the simulation model with the number of chargers ranging from one to 10 (with a step size of one), the charging power ranging from 20 kW to 100 kW (with a step size of 20 kW), and a battery capacity of 100 kWh. Fig. 12 shows the average daily miles driven by all CNG buses with different numbers of chargers and different charging powers. From Fig. 12, two interesting observations can be made. First, when the number of chargers is fixed, the average daily miles traveled by CNG buses decreases with increasing charging power. Second, for a given charging power, the average daily miles traveled by CNG buses tends to decrease as the number of chargers increases. Take the 40-kW case as an example. The average daily miles traveled by CNG buses first decreases as the number of chargers increases from one to four, then fluctuates within a small range when the number of chargers increases from four to 10. These results are expected because with more chargers and higher charging power, e-buses can reduce their charging and queueing times at the charging station and replace more miles traveled by CNG buses. For a certain charging power, when the number of chargers increases to a certain critical value, further increasing the number of chargers will no longer significantly reduce the miles traveled by CNG buses. The critical number of chargers is 7 for the 20-kW case, 4 for the 40-kW case, 4 for the 60-kW case, 3 for the 80-kW case, and 3 for the 100-kW case. The fluctuation in the average daily miles traveled by CNG buses after the number of chargers reaches the critical value is most likely due to the stochastic features of the simulation.

4.3. System optimization

In this section, we optimize the design of the airport bus system using the simulation-based optimization model. In Section 4.3.1, we consider a scenario where 10 CNG buses are replaced by battery e-buses. Then, in Section 4.3.2, we investigate the impact of the distance between the rental car center and the charging station. Section 4.3.3 considers

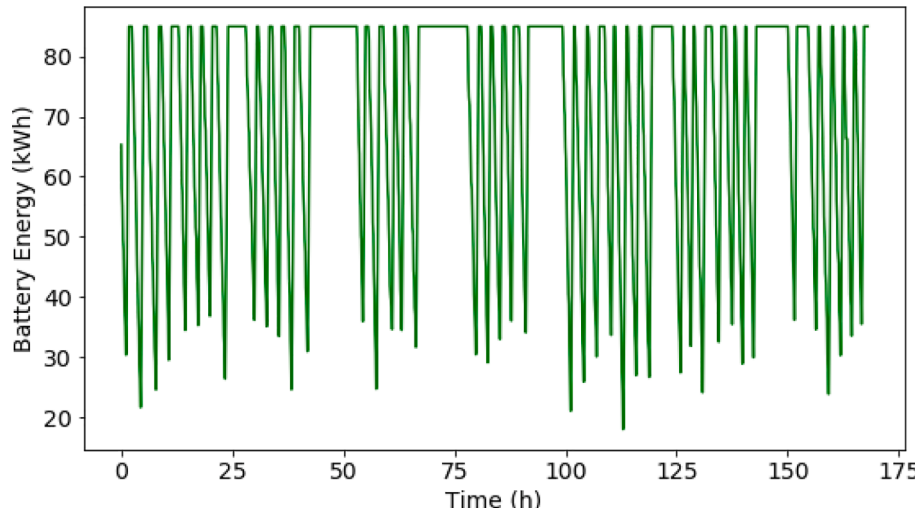


Fig. 8. Sample SoC profile of an e-bus.

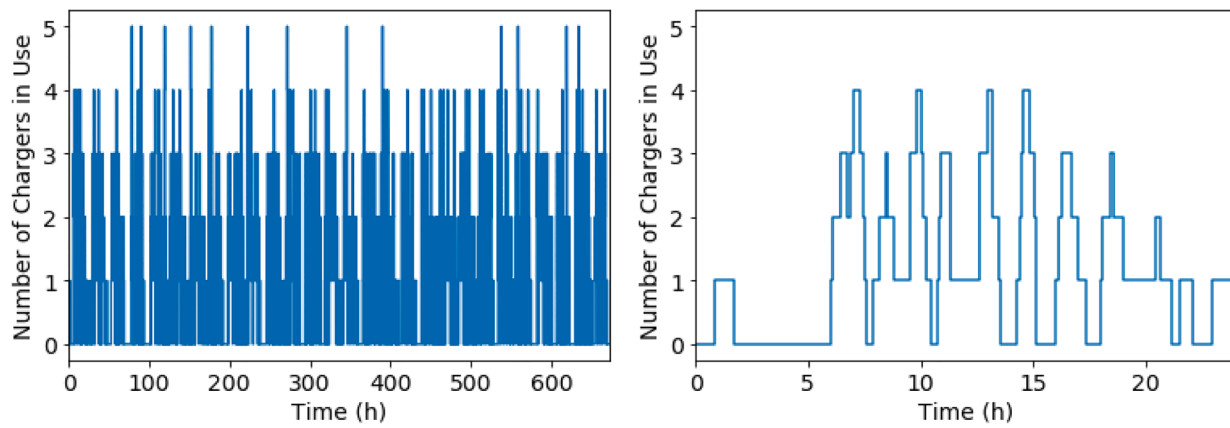


Fig. 9. Charger usage profile.

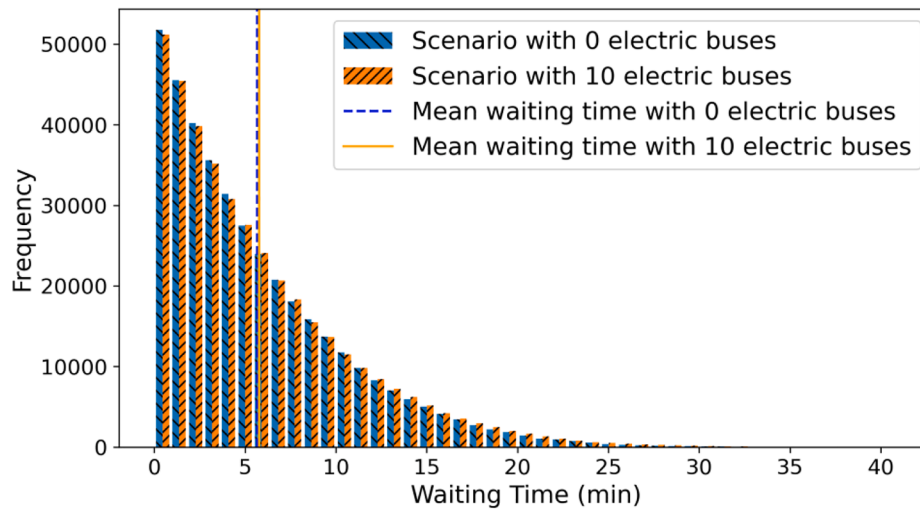


Fig. 10. Histograms of passenger waiting times with zero and 10 e-buses.

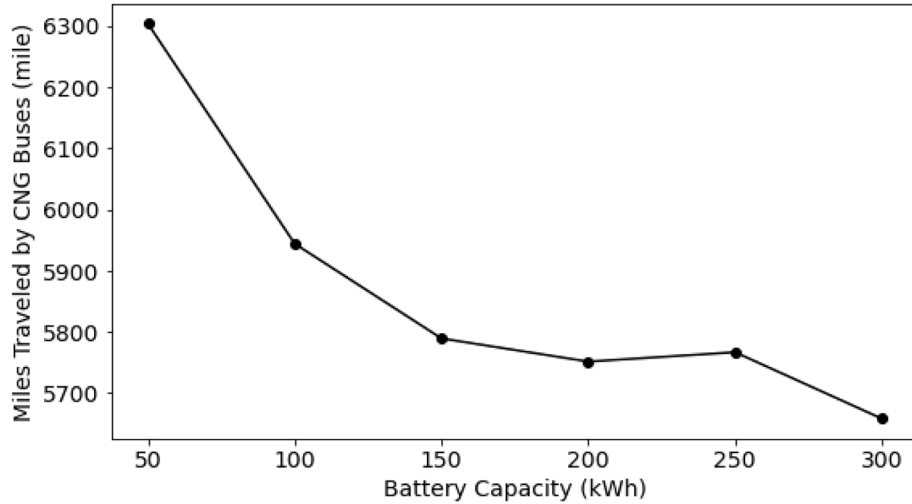


Fig. 11. Average daily miles traveled by CNG buses given different e-bus battery capacities.

another two scenarios where 20 and 30 CNG buses are replaced by e-buses. In Section 4.3.4, we introduce a flexible charging strategy and test its potential impact on optimal system design. Lastly, in Section 4.3.5, we consider a full fleet electrification scenario and use the genetic-

algorithm-based solution procedure discussed in Section 3.2 to solve the system optimization problem.

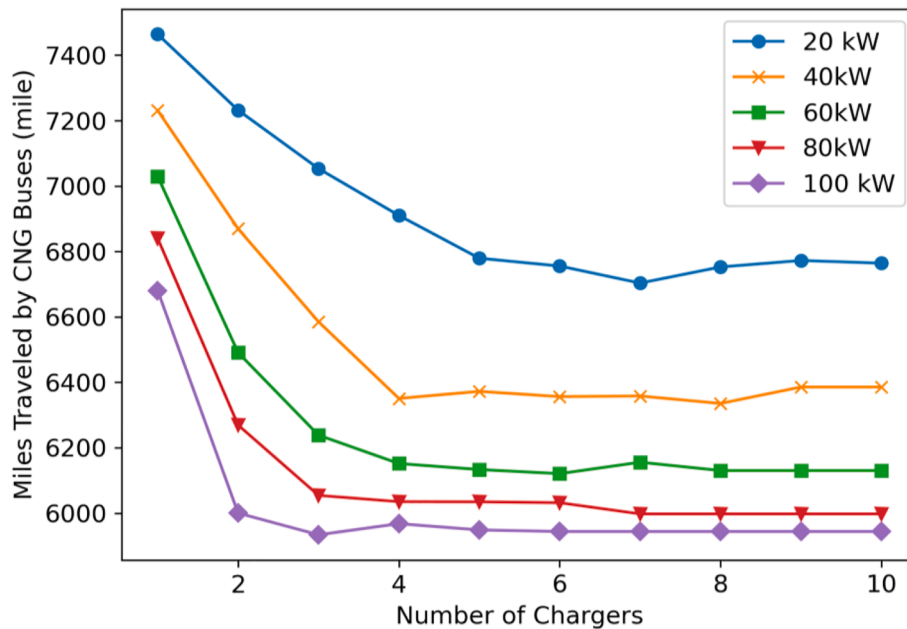


Fig. 12. Average daily miles traveled by CNG buses with different numbers of chargers and different charging powers.

4.3.1. Scenario with 10 electric buses

In this section, we assume that DFW plans to convert 10 CNG buses into battery e-buses. As shown in Section 4.2, using larger battery capacities and installing more high-power chargers can reduce the miles traveled by CNG buses. However, using large battery capacities and installing many high-power chargers requires significant capital cost. Therefore, a tradeoff must be made between the capital cost of deploying e-buses and the bus system performance. To help DFW determine the best tradeoff, we consider a bi-objective version of the optimization problem presented in Section 3.2, where the two objectives are to minimize the capital cost and minimize the miles traveled by CNG buses. The second objective can be viewed as minimizing greenhouse gas emissions.

The charger cost is set to \$350/kW [44]. The charging efficiency of the chargers is set to 91.4 % [43]. The distance between the rental car center and the charging station is set to 2.5 miles. The vehicle cost of an

e-bus (excluding the battery) is set to \$550,000, and the battery cost is set to \$500/kWh, including midlife replacement [45]. Because 10 e-buses will be deployed, the maximum number of chargers is 10, i.e., $x \in \{1, 2, \dots, 10\}$. We consider 35 possible charging powers from 10 kW to 350 kW, with a step size of 10 kW, i.e., $\sigma \in \{10, 20, \dots, 350\}$. For battery capacity, we consider 12 possible choices from 50 kWh to 600 kWh, with a step size of 50 kWh, i.e., $e^{max} \in \{50, 100, \dots, 600\}$. In total, there are 4,200 combinations of the number of chargers, charging powers, and battery capacities. Using Message Passing Interface (MPI), a standardized and portable message-passing standard designed to function on parallel computing architectures, on NREL's high-performance computing system, Eagle, we ran all 4,200 simulations in parallel using 600 processors. Running all the simulations and collecting the miles traveled by CNG buses took approximately 20 min.

Fig. 13 shows the capital cost and average daily miles traveled by CNG buses for both nondominated (Pareto optimal) solutions (marked

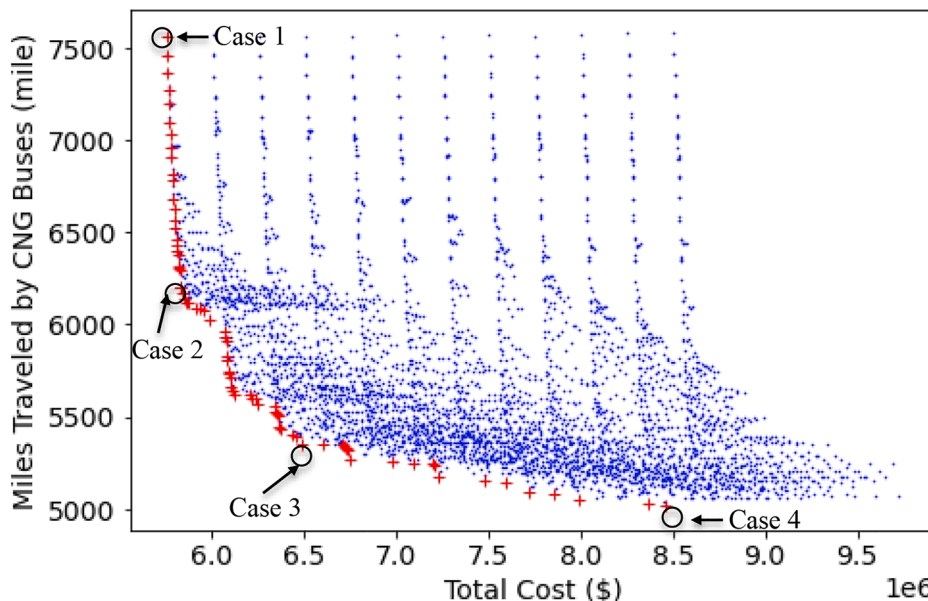


Fig. 13. The capital cost and average daily miles traveled by CNG buses for nondominated and dominated solutions.

using a red “+”) and dominated solutions (marked using a blue “•”). As shown in the figure, the Pareto optimal solutions define a boundary beyond which neither of the two objectives (reducing average daily miles traveled by CNG buses and reducing the total capital cost) can be further improved without compromising the other objective. These Pareto optimal solutions can offer useful guidance to DFW for deploying the 10 e-buses to achieve a balanced tradeoff between the two objectives. Four representative solutions are highlighted in Fig. 13. The corresponding battery capacities, charging powers, and numbers of chargers are reported in Table 2.

Solution 1 provides a design with minimal capital cost and maximal miles traveled by CNG buses. With only one 10-kW charger deployed, the 10 e-buses will spend a lot of time waiting and charging at the charging station. In addition, with a small 50-kWh battery capacity, the e-buses will require frequent charging during operation and will waste lots of time traveling between the rental car center and the charging station. Among all the Pareto optimal solutions, solution 4 provides a design with the minimal miles traveled by CNG buses and the maximal capital cost. Using a 500-kWh battery capacity and four 330-kW chargers, e-buses can be efficiently utilized to reduce the miles traveled by CNG buses. Compared to solutions 1 and 4, solutions 2 and 3 provide a more balanced tradeoff between the two objectives.

From solution 1 to solution 2, although the battery capacity and the number of chargers remains unchanged, the increase of charging power from 10 kW to 230 kW significantly reduces the queuing and charging time of e-buses at the charging station. Consequently, the average daily miles traveled by CNG buses drops from 7,563 to 6,204, a reduction of 20 %, while the capital cost only increases from \$5,753,500 to \$5,830,500, an increase of 1 %.

Compared to solution 2, solution 3 utilizes a larger battery capacity to reduce the deadhead travel between the rental car center and the charging station. Additionally, it installs more high-power chargers to further reduce the queuing and charging time. From solution 2 to solution 3, the average daily miles traveled by CNG buses drops from 6,204 to 5,353, a reduction of 14 %, while the capital cost increases from \$5,830,500 to \$6,488,000, an increase of 11 %.

From solution 3 to solution 4, the average daily miles traveled by CNG buses can further be reduced from 5,353 to 5,015, a reduction of 6 %. However, this improvement requires a capital cost increase from \$6,488,000 to \$8,462,000, an increase of 30 %.

4.3.2. Impact of the distance to the charging station

If the charging station is far from the rental car center, the deadhead travel of e-buses between the charging station and the rental car center will waste service time and energy. To investigate the impact of the distance between the charging station and the rental car center on the performance of a bus system design, we performed a sensitivity analysis by solving the above bi-objective optimization problem with the distance ranging from zero miles to 10 miles with a step size of 2.5 miles. Note that the zero-mile case means that chargers are installed at the rental car center. Fig. 14 shows the Pareto frontiers with different distances between the charging station and the rental car center.

One can observe from Fig. 14 that with the decrease in the distance between the charging station and the rental car center, the corresponding Pareto frontier moves toward the lower left. The closer the

Table 2

Detailed Information on the Four Representative Solutions.

Solution	Battery Size (kWh)	Charging Power (kW)	Number of Chargers	Total Capital Cost (\$)	Average Daily Miles by CNG Buses (miles)
1	50	10	1	5,753,500	7563
2	50	230	1	5,830,500	6204
3	150	340	2	6,488,000	5353
4	500	330	4	8,462,000	5015

Pareto frontier gets to the lower-left corner (i.e., smaller capital cost and average daily miles traveled by CNG buses) the better; thus, the results imply that bus system designs with shorter distances between the charging station and the rental car center can achieve better performance.

4.3.3. Scenarios with 20 and 30 electric buses

We further consider another two scenarios where 20 and 30 CNG buses are replaced by battery e-buses. The maximum number of chargers for each scenario equals the number of e-buses. The distance between the rental car center and the charging station is set to 2.5 miles. In addition to the two objectives, i.e., minimizing the capital cost and minimizing the miles traveled by CNG buses, we also consider a constraint that ensures the mean waiting time for passengers using the bus system meets the existing level of service. Under the status quo scenario, i.e., with no e-buses, the mean waiting time for passengers is 355 s. Thus, a feasible solution should ensure that passengers' mean waiting time for the designed bus system is no greater than the 355 s.

Fig. 15 and Fig. 16 show the capital cost and average daily miles traveled by CNG buses for both nondominated (Pareto optimal) solutions (marked using a red “+”) and dominated solutions (marked using a blue “•”) under the 20 and 30 e-bus scenarios, respectively. Two extreme solutions are highlighted in the corresponding figure for each scenario. For both scenarios, solution 1 is the Pareto optimal solution with the minimum capital cost, and solution 2 is the Pareto optimal solution with the minimum CNG bus miles. Table 3 and Table 4 provide detailed information about the two extreme solutions for the 20 and 30 e-bus scenarios, respectively. One can observe from Fig. 13, Fig. 15, and Fig. 16 that the three Pareto frontiers have a similar shape. From solution 1 in Table 3, one can observe that, under the scenario with 20 e-buses, the bus system can still ensure that passengers' waiting time is less than 355 s, even with only one 10-kW charger installed. However, under the scenario with 30 e-buses, at least one 330-kW charger is required to ensure the feasibility of the design (i.e., a waiting time of less than 355 s), as shown by solution 1 in Table 4. Solution 2 for the scenario with 20 e-buses (Table 3) shows that with more capital investment, the average daily miles traveled by CNG buses can be reduced to 2,582 miles. For the scenario with 30 e-buses, solution 2 (Table 4) shows that the average daily miles traveled by CNG buses can be further reduced to 505 miles.

4.3.4. Flexible charging strategy

In the simulation results presented in Section 4.2 and Sections 4.3.1–4.3.3, we assumed that an e-bus would charge its battery when its SoC fell below a prespecified lower bound. In this section, we consider a more flexible charging strategy. Here, we assume chargers are installed at the rental car center. For this flexible charging strategy, we define another threshold for battery SoC, termed the *flexible charging threshold*, that specifies the charging behavior of each e-bus as follows. When an e-bus returns to the rental car center, it will check its battery SoC; if the expected battery SoC after finishing the next trip falls below the SoC lower bound, the e-bus must go charge. However, if the expected battery SoC after finishing the next trip is above the SoC lower bound but the current SoC falls below the flexible charging threshold, the e-bus will go charge if there is a charger available, or, if no charger is available, it will continue serving the next trip. Note that the flexible charging threshold should be larger than the SoC lower bound. To test this flexible charging strategy, we solved the system optimization problems, including optimizing over the flexible charging strategy, for the three scenarios with 10, 20, and 30 e-buses. We consider 7 possible values for the flexible charging threshold ranging from 0.2 to 0.8, with a step size of 0.1. Figs. 17–19 compare the Pareto frontiers with and without flexible charging under the three scenarios with 10, 20, and 30 e-buses, respectively. For each scenario, the Pareto frontier for the flexible charging strategy case is closer to the lower-left corner compared to the case without flexible charging. Because smaller capital cost and average

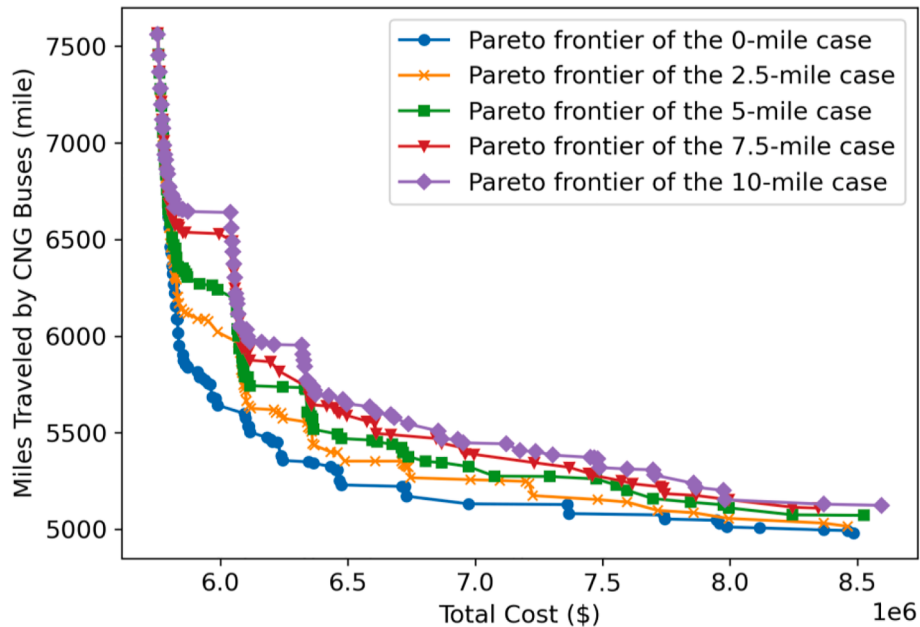


Fig. 14. Pareto frontiers with different distances between the rental car center and the charging station.

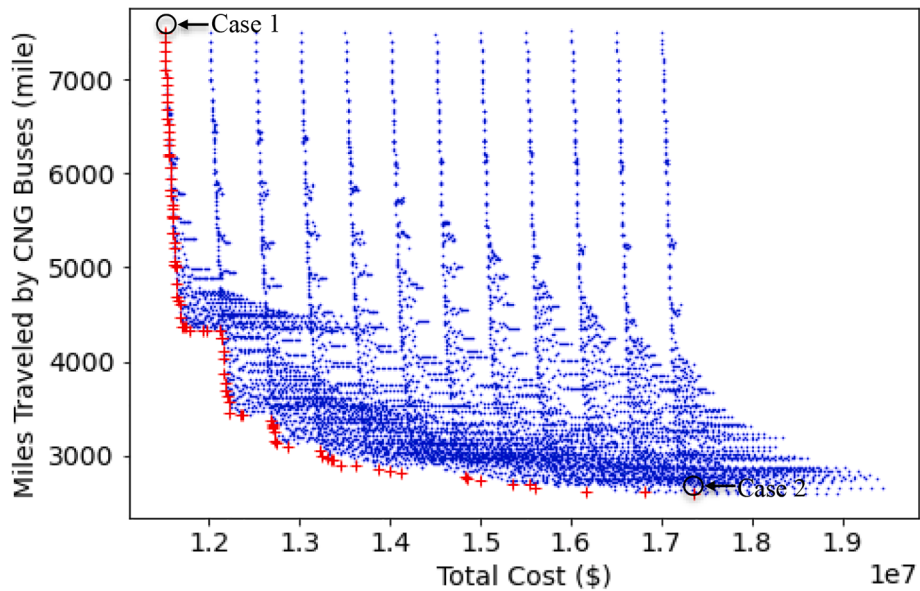


Fig. 15. The capital cost and average daily miles traveled by CNG buses for nondominated and dominated solutions under the scenario with 20 e-buses.

daily miles traveled by CNG buses can be achieved as the Pareto frontier gets closer to the lower-left corner, these results imply that the bus system design with the flexible charging strategy has better performance than the design without the flexible charging strategy. The benefits of incorporating a flexible charging strategy can be significant under certain scenarios. As shown in the Fig. 19, if decision-makers want to have NonEV miles (miles traveled by CNG buses) at the level marked by the dotted line, the scenario without flexible charging will cost about \$22.2 million, whereas the scenario with flexible charging can reduce the cost to \$20.1 million, a 9.5 % reduction. In practice, however, DFW should further consider the tradeoff between the benefit of the flexible charging strategy and the difficulty and/or cost of implementing it, which is beyond the scope of this study.

4.3.5. Full fleet electrification

Now, we consider the case where DFW replaces all CNG buses with e-

buses, with a goal of minimizing the total capital cost while ensuring that passengers' mean waiting time is no greater than the 355-second waiting time under the status quo scenario. Because the fleet size of the shuttle system is 46, the number of chargers can range from 1 to 46, i.e., $x \in \{1, 2, \dots, 46\}$. The possible values for charging power and battery capacity are the same as those in Section 4.3.1, i.e., $\sigma \in \{10, 20, \dots, 350\}$ and $e^{max} \in \{50, 100, \dots, 600\}$. We assume that chargers are installed at the rental car center. The flexible charging strategy from Section 4.3.4 is also considered, with the flexible charging threshold ranging from 0.2 to 0.8 with a step size of 0.1. In total, there are 135,240 combinations of the number of chargers, charging powers, battery capacities, and the flexible charging threshold. We solved the system optimization problem using the proposed genetic-algorithm-based solution procedure with $pop_size = 100$, $Prob_co = 0.6$, $Prob_mt = 0.15$, and $max_generation = 150$. At each iteration, 100 processors were used to run the simulation for each chromosome in parallel. It took

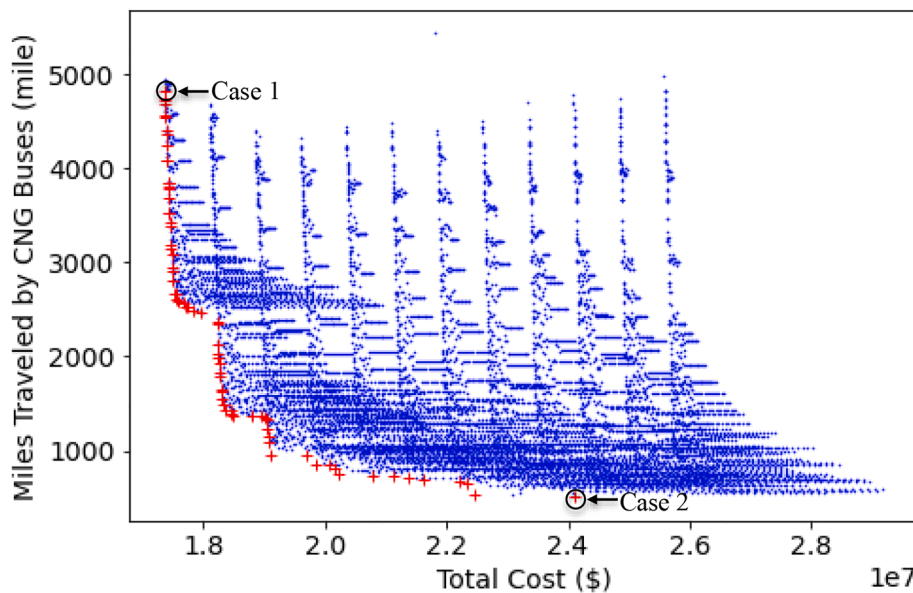


Fig. 16. The capital cost and average daily miles traveled by CNG buses for nondominated and dominated solutions under the scenario with 30 e-buses.

Table 3
Detailed Information About the Two Representative Solutions for the Scenario With 20 E-Buses.

Solution	Battery Size (kWh)	Charging Power (kW)	Number of Chargers	Total Capital Cost (\$)	Average Daily Miles by CNG Buses (miles)
1	50	10	1	11,503,500	7511
2	550	350	7	17,357,500	2582

Table 4
Detailed Information About the Two Representative Solutions for the Scenario With 30 E-Buses.

Solution	Battery Size (kWh)	Charging Power (kW)	Number of Chargers	Total Capital Cost (\$)	Average Daily Miles by CNG Buses (miles)
1	50	330	1	17,365,500	4715
2	450	350	7	24,107,500	505

approximately 10 h to finish the solution procedure. Fig. 20 shows the convergence performance of the parallel genetic-algorithm-based solution procedure. Note that the constant vehicle cost is excluded from the total cost. The obtained solution is reported as follows: battery capacity $e^{max} = 50$ kWh, charging power $\sigma = 210$ kW, number of chargers $x = 4$, and flexible charging threshold = 0.2. The total capital cost is \$26,744,000, which consists of total battery and charger costs of \$1,444,000 and constant vehicle costs of \$25,300,000. The mean waiting time for passengers is 353 s, which is below the 355-second waiting time under the status quo scenario. To further verify the effectiveness of the genetic-algorithm-based solution procedure, we simulated and evaluated all 135,240 combinations of the number of chargers, charging powers, battery capacities, and the flexible charging threshold. Fig. 21 shows the mean waiting times and total battery and charger costs for all feasible solutions. One can observe that the solution obtained from the genetic-algorithm-based procedure (highlighted using a red "x") is the global optimal solution, demonstrating the effectiveness of the solution procedure.

4.3.6. Comparison with existing methods

To the best of our knowledge, there are no existing studies that address the planning problem of airport e-bus systems with station-based charging. However, as discussed in the Introduction, a few studies have developed mathematical programs to investigate the planning problem of city e-bus systems with station-based charging (e.g., [11,18,17]). Compared to existing studies that optimize e-bus system design using pure mathematical programs, the proposed simulation-based optimization framework can depict the real-world operation of an e-bus system with much higher fidelity. To ensure tractability, mathematical programs usually simplify the operation of an e-bus system. For instance, none of the aforementioned studies consider bus capacity, passenger queuing behavior at bus stops, and e-bus queuing behavior at charging stations. In our simulation-based optimization framework, each system design is evaluated using a high-fidelity simulation driven by real-world operation data, which is close to a real-world field test. Therefore, optimal solutions from our framework should always have performance that is equal to or better than solutions from pure mathematical programs. The downside of the simulation-based optimization framework is that the simulation model requires abundant bus operation data and lots of computing resources. For complex city bus systems with a lot of bus routes, many shared terminals and transfer bus stops, and massive passenger origin–destination pairs, the simulation-based method might be computationally too expensive, compelling us to rely on simplified mathematical programs to address the planning problem. Compared to city bus systems, airport shuttle systems usually have a much simpler structure and passenger demands. Our numerical studies demonstrate that the computational burden of the proposed simulation-based optimization framework is acceptable for a real-world airport shuttle system.

4.3.7. Battery degradation and Grid-Side effect of charging

The capacity of e-bus batteries degrades over time and during the charging and discharging cycles. Battery aging is impacted by many correlated factors, such as depth of discharge, environmental conditions, temperature, the quality of the chemical elements used to manufacture the battery, fast/slow charging, etc. It is therefore difficult to accurately estimate battery aging. In practice, when the capacity of a battery drops by more than 20 % or the internal resistance doubles, the battery will be replaced with a new one [46]. In the literature, studies on e-bus system planning usually consider a midlife battery replacement cost. The battery cost used in our numerical studies is set to \$500/kWh, including

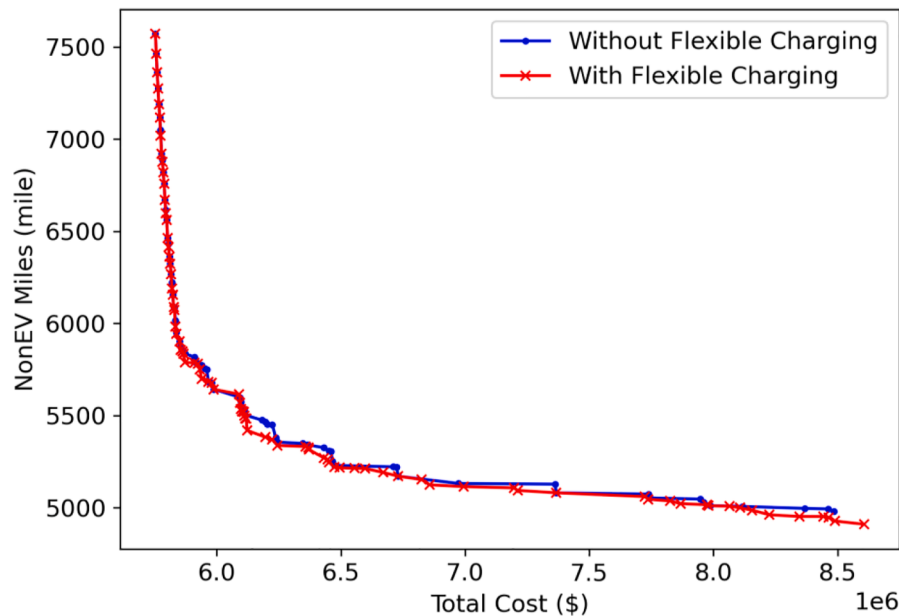


Fig. 17. Comparison between Pareto frontiers with and without flexible charging under the scenario with 10 e-buses.

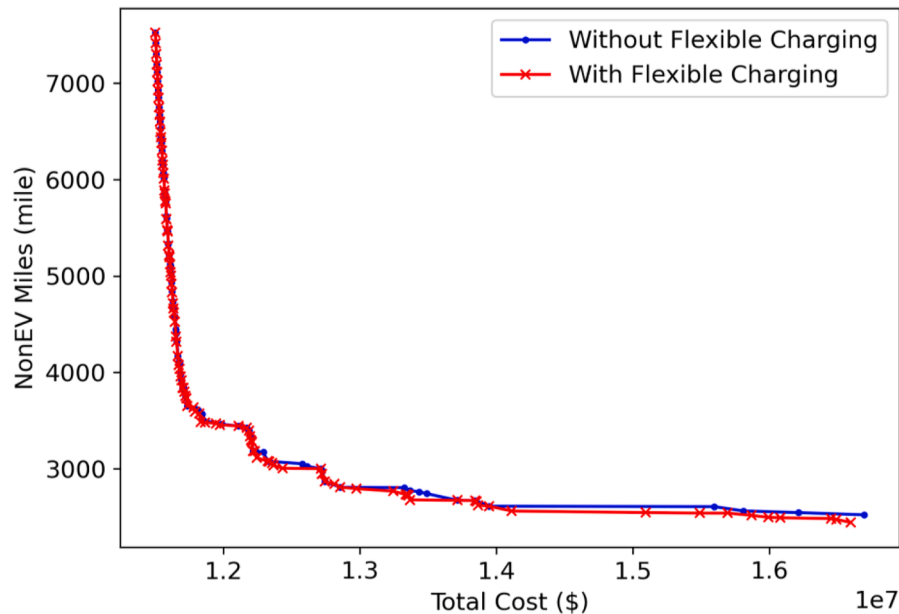


Fig. 18. Comparison between Pareto frontiers with and without flexible charging under the scenario with 20 e-buses.

midlife replacement [45]. To consider the worst-case scenario when the battery capacity drops 20 % before replacement, we can add an 80 % coefficient to battery capacity in the simulation to ensure normal shuttle system operation. Simulation results show that, with full fleet electrification, the solution with a 50-kWh battery capacity and four 210-kW chargers is still the optimal solution, meaning that the 50-kWh nominal battery capacity is large enough to ensure normal operation even when it drops by 20 %.

Probable grid impacts of electric vehicle charging include peak power demand increases, regulatory voltage limit violations, power loss increases, distribution system asset overloading, harmonic problems, and system voltage stability issues [47]. Installing energy storage units at the fast charging station [48] and incorporating smart charging scheduling and management [49] are two potential ways to alleviate the impact of e-bus fast charging on the power grid.

5. Conclusions

In this study, we address the strategic planning problem for electric airport shuttle systems. We develop a data-driven simulation-based optimization modeling framework to help airport shuttle system operators who plan to deploy e-buses determine the battery capacity, charging power, and number of chargers to be installed. Compared to existing studies, the primary contribution of the proposed method is that it can model the real-world stochastic nature of e-bus system operations with much higher fidelity.

The effectiveness of the proposed model is demonstrated through extensive numerical studies based on a real-world airport shuttle system that connects the five terminals and the rental car center at DFW. When the airport shuttle system is partially electrified, the simulation-based optimization model considers two objectives—minimizing the total

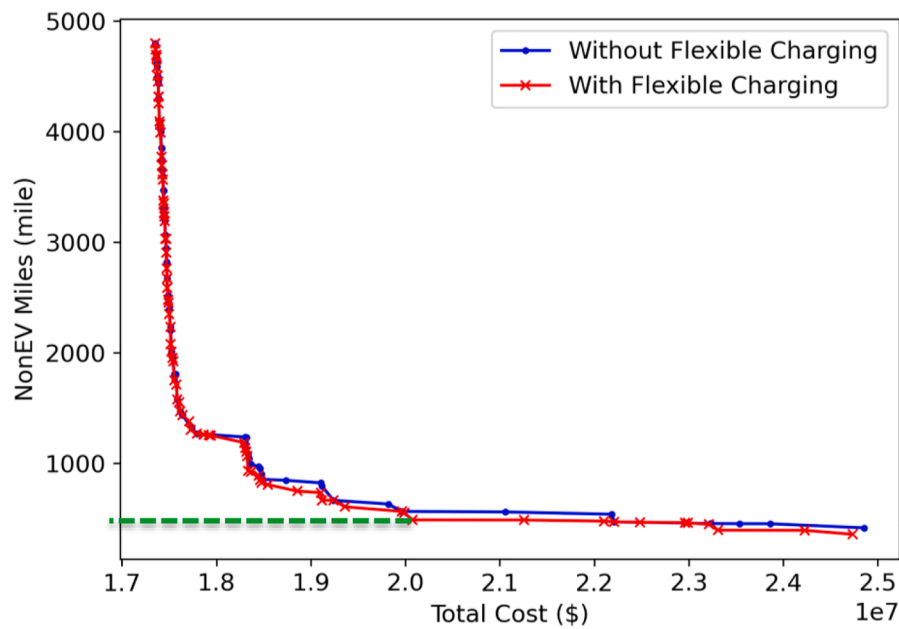


Fig. 19. Comparison between Pareto frontiers with and without flexible charging under the scenario with 30 e-buses.

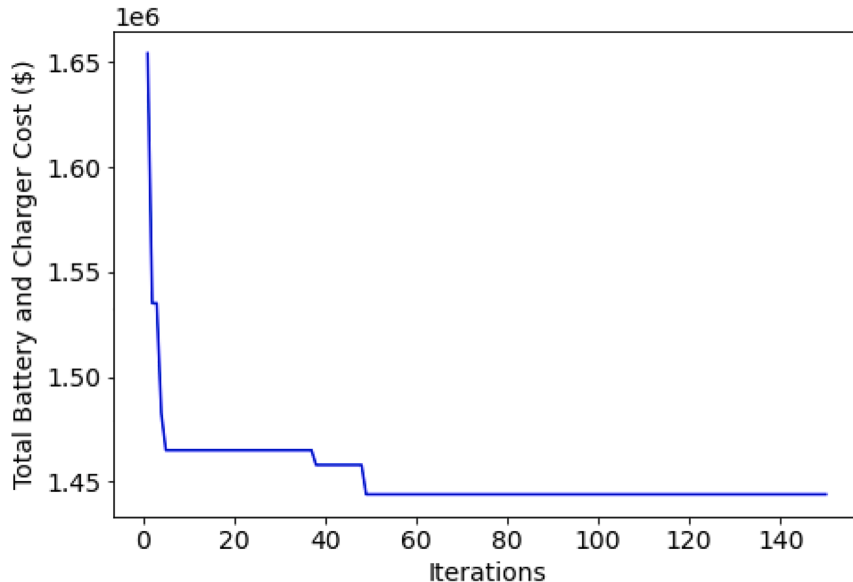


Fig. 20. Convergence of the genetic-algorithm-based solution procedure.

capital cost and minimizing the average daily miles traveled by CNG buses—and provides a set of Pareto optimal solutions. For instance, when 10 buses are electrified, the solution with a 50-kWh battery capacity and one 10-kW charger leads to the minimum capital cost and the maximal miles traveled by CNG buses; the solution with a 500-kWh battery capacity and four 330-kW chargers has the minimal miles traveled by CNG buses and the maximal capital cost; and other Pareto optimal solutions provide different tradeoffs between the two objectives. When considering full fleet electrification, the model finds a solution that minimizes the total capital cost while ensuring that the passengers' mean waiting time does not exceed the one under the status quo scenario. The solution requires a 50-kWh battery capacity and four 210-kW chargers, resulting in a total capital cost of \$26,744,000. Brute force enumeration can find global optimal solution(s) but requires massive computing resources to evaluate all possible solutions. The proposed genetic-algorithm-based solution procedure can effectively

find near-optimal solutions with limited computing resources.

Concerns about air quality impacts and regulations will drive more and more airports to convert their shuttle fleets to zero-emission e-buses. The proposed modeling framework can provide practitioners with an effective tool for the strategic planning of an electric airport shuttle system.

Numerical studies provided in this paper are based on the data collected in wintertime, which might not capture the potentially higher energy consumption from air-conditioning during the summer months. Two potential methods might be used in future studies to address this limitation. First, if possible, shuttle bus operation data during the summer months should be collected to capture the bus energy consumption characteristics during summertime. Second, a thermal cabin model can be developed to estimate the air-conditioning energy consumption under different ambient temperatures. This study only considers a fixed number of buses being replaced by e-buses and does not

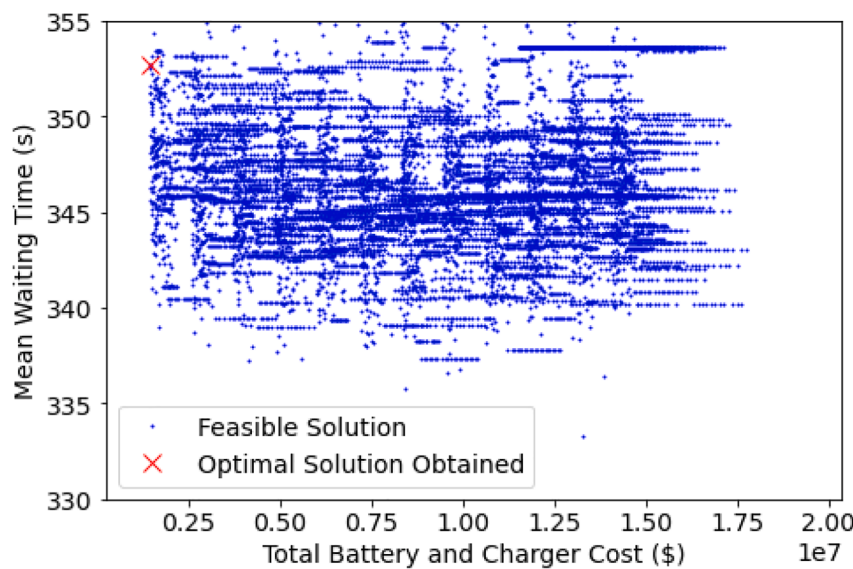


Fig. 21. Illustration of the optimality of the obtained solution.

consider gradual implementation of e-buses. Our future research will consider time-dependent gradual electrification of an airport bus system, in which the number of e-buses to be deployed at each planning period is also a decision variable. We will also investigate other charging technologies (e.g., battery swapping and dynamic wireless charging) in airport shuttle systems in future studies.

CRediT authorship contribution statement

Zhaocai Liu: Conceptualization, Data curation, Methodology, Formal analysis, Writing - original draft. **Qichao Wang:** Conceptualization, Data curation, Methodology, Formal analysis, Writing - original draft. **Devon Sigler:** Conceptualization, Data curation, Formal analysis, Writing - original draft. **Andrew Kotz:** Conceptualization, Data curation, Writing - original draft. **Kenneth J. Kelly:** Conceptualization. **Monte Lunacek:** Conceptualization, Project administration. **Caleb Phillips:** Conceptualization, Funding acquisition. **Venu Garikapati:** Conceptualization.

Declaration of Competing Interest

The authors declare that they have no known competing financial interests or personal relationships that could have appeared to influence the work reported in this paper.

Data availability

The authors do not have permission to share data.

Acknowledgment

This work was supported by the U.S. Department of Energy (U.S. DOE) and Dallas Fort-Worth International Airport (DFW). This work was authored in part by the National Renewable Energy Laboratory, operated by Alliance for Sustainable Energy, LLC, for the U.S. Department of Energy (DOE) under Contract No. DE-AC36-08GO28308. The contents of this paper reflect the view of the authors who are responsible for the facts and accuracy of the data presented herein. The contents do not necessarily reflect the official view or policies of the U.S. DOE. The U.S. Government retains and the publisher, by accepting the article for publication, acknowledges that the U.S. Government retains a non-exclusive, paid-up, irrevocable, worldwide license to publish or reproduce the published form of this work, or allow others to do so, for U.S.

Government purposes.

References

- [1] Burd JTJ, Moore EA, Ezzat H, Kirchain R, Roth R. Improvements in electric vehicle battery technology influence vehicle lightweighting and material substitution decisions. *Appl Energy* 2021;283:116269.
- [2] Baars J, Domenech T, Bleischwitz R, Melin HE, Heidrich O. Circular economy strategies for electric vehicle batteries reduce reliance on raw materials. *Nat Sustainability* 2021;4(1):71–9.
- [3] Nezamuddin ON, Nicholas CL, dos Santos EC. The Problem of Electric Vehicle Charging: State-of-the-Art and an Innovative Solution. *IEEE Trans Intell Transp Syst* 2021.
- [4] Eltoumi FM, Becherif M, Djerdir A, Ramadan HS. The key issues of electric vehicle charging via hybrid power sources: Techno-economic viability, analysis, and recommendations. *Renew Sustain Energy Rev* 2021;138:110534.
- [5] Rajendran G, Vaithilingam CA, Misron N, Naidu K, Ahmed MR. A comprehensive review on system architecture and international standards for electric vehicle charging stations. *J Storage Mater* 2021;42:103099.
- [6] Ding X, Wang Z, Zhang L. Hybrid control-based acceleration slip regulation for four-wheel-independent-actuated electric vehicles. *IEEE Trans Transp Electrif* 2020;7(3):1976–89.
- [7] Ding X, Wang Z, & Zhang L. (2020b, November). A Vehicle Rollover Prediction System Based on Lateral Load Transfer Ratio. In 2020 Chinese Automation Congress (CAC) (pp. 7256–7261). IEEE.
- [8] Akhtar N, Patil V. Electric Vehicle Technology: Trends and Challenges. In: *In Smart Technologies for Energy, Environment and Sustainable Development*. Singapore: Springer; 2022. p. 621–37.
- [9] Ding X, Wang Z, Zhang L. Event-triggered vehicle sideslip angle estimation based on low-cost sensors. *IEEE Trans Ind Inf* 2021.
- [10] Mustafi NN. An Overview of Hybrid Electric Vehicle Technology. *Engines and Fuels for Future Transport* 2022:73–102.
- [11] Kunith A, Mendelevitch R, Goehlich D. Electrification of a city bus network—An optimization model for cost-effective placing of charging infrastructure and battery sizing of fast-charging electric bus systems. *Int J Sustain Transp* 2017;11(10):707–20.
- [12] Helber S, Broihan J, Jang YJ, Hecker P, Feuerle T. Location planning for dynamic wireless charging systems for electric airport passenger buses. *Energies* 2018;11(2):258.
- [13] Lin Y, Zhang K, Shen M, Ye B, Miao L. Multistage large-scale charging station planning for electric buses considering transportation network and power grid. *Transp Res Part C* 2019;107:423–43.
- [14] Margolis J. 2019. China dominates the electric bus market, but the US is getting on board. <https://www.pri.org/stories/2019-10-08/china-dominates-electric-bus-market-us-getting-board> (Accessed July 2021).
- [15] Green Car Congress. Number of electric buses in Europe has increased from around 200 to 2,200 in 5 years. Accessed July 2021, <https://www.greencarcongress.com/2019/10/20191020-busworld.html>; 2019.
- [16] Federal Transit Administration. Low or No-Emission (Low-No) Bus Program Projects. Accessed July 2021, <https://search.usa.gov/search?utf8=%E2%9C%93&affiliate=dot-fta&query=low+or+No-Emission+%28Low-No%29+Bus+Program+Project+;> 2021.
- [17] An K. Battery electric bus infrastructure planning under demand uncertainty. *Transp Res Part C* 2020;111:572–87.

- [18] Liu Z, Song Z, He Y. Planning of fast-charging stations for a battery electric bus system under energy consumption uncertainty. *Transp Res Record* 2018;2672(8):96–107.
- [19] Nunno R. 2018. Fact Sheet: Battery Electric Buses: Benefits Outweigh Costs. <https://www.eesi.org/papers/view/fact-sheet-electric-buses-benefits-outweigh-costs> (Accessed July 2021).
- [20] Chen Z, Yin Y, Song Z. A cost-competitiveness analysis of charging infrastructure for electric bus operations. *Transp Res Part C* 2018;93:351–66.
- [21] Li JQ. Battery-electric transit bus developments and operations: A review. *Int J Sustain Transp* 2016;10(3):157–69.
- [22] An K, Jing W, Kim I. Battery-swapping facility planning for electric buses with local charging systems. *Int J Sustain Transp* 2020;14(7):489–502.
- [23] Ko YD, Jang YJ. The optimal system design of the online electric vehicle utilizing wireless power transmission technology. *IEEE Trans Intell Transp Syst* 2013;14(3):1255–65.
- [24] Jang YJ, Jeong S, Ko YD. System optimization of the on-line electric vehicle operating in a closed environment. *Comput Ind Eng* 2015;80:222–35.
- [25] Hwang I, Jang YJ, Ko YD, Lee MS. System optimization for dynamic wireless charging electric vehicles operating in a multiple-route environment. *IEEE Trans Intell Transp Syst* 2017;19(6):1709–26.
- [26] Liu Z, Song Z, He Y. Optimal deployment of dynamic wireless charging facilities for an electric bus system. *Transp Res Record* 2017;2647(1):100–8.
- [27] Liu Z, Song Z. Robust planning of dynamic wireless charging infrastructure for battery electric buses. *Transp Res Part C* 2017;83:77–103.
- [28] Alwesabi Y, Avishan F, Yanıkoglu İ, Liu Z, Wang Y. Robust strategic planning of dynamic wireless charging infrastructure for electric buses. *Appl Energy* 2022;307:118243.
- [29] Bi Z, Keoleian GA, Ersal T. Wireless charger deployment for an electric bus network: A multi-objective life cycle optimization. *Appl Energy* 2018;225:1090–101.
- [30] Bi Z, Song L, De Kleine R, Mi CC, Keoleian GA. Plug-in vs. wireless charging: Life cycle energy and greenhouse gas emissions for an electric bus system. *Appl Energy* 2015;146:11–9.
- [31] Bi Z, Kan T, Mi CC, Zhang Y, Zhao Z, Keoleian GA. A review of wireless power transfer for electric vehicles: Prospects to enhance sustainable mobility. *Appl Energy* 2016;179:413–25.
- [32] Jang YJ. Survey of the operation and system study on wireless charging electric vehicle systems. *Transportation Research Part C: Emerging Technologies* 2018;95:844–66.
- [33] Brenna M, Foiadelli F, Leone C, Longo M. Electric vehicles charging technology review and optimal size estimation. *J Electr Eng Technol* 2020;15(6):2539–52.
- [34] Rogge M, Van der Hurk E, Larsen A, Sauer DU. Electric bus fleet size and mix problem with optimization of charging infrastructure. *Appl Energy* 2018;211:282–95.
- [35] Lawrence, 2020. Electric Shuttles are Taking Off at Airports. <https://www.act-news.com/news/electric-shuttles-are-taking-off-at-airports/> (Accessed July 2021).
- [36] Wang Q, Sigler D, Kotz A, Liu Z, Kelly K. and Phillips C. 2021. ASPIRES: Airport Shuttle Planning and Improved Routing Event-driven Simulation <https://github.com/NREL/athena-aspires>. (Accessed Oct 2022).
- [37] Wang Q, Sigler D, Liu Z, Kotz A, Kelly K, Phillips C. ASPIRES: Airport Shuttle Planning and Improved Routing Event-driven Simulation. *Transp Res Rec* 2022. <https://doi.org/10.1177/03611981221095744>.
- [38] Sigler D, Wang Q, Liu Z, Garikapati V, Kotz A, Kelly KJ, Lunacek M, Phillips C. Route optimization for energy efficient airport shuttle operations—A case study from Dallas Fort Worth International Airport. *J Air Transp Manag* 2021;94:102077.
- [39] Matloff N. Introduction to discrete-event simulation and the simpy language 2008; 2:1–33. Retrieved on August.
- [40] Nelson B. Foundations and methods of stochastic simulation: a first course. Springer Science & Business Media; 2013.
- [41] Patil VP, Pawar DD. The optimal crossover or mutation rates in genetic algorithm: a review. *International Journal of Applied Engineering and Technology* 2015;5(3):38–41.
- [42] Kotz J, Licenec K, Kelly KJ, Berger S. Electrification of Airport Shuttle Operations. 33rd Electric Vehicle Symposium. 2020.
- [43] Johnson C, Nobler E, Eudy L. and Jeffers M. 2020. Financial Analysis of Battery Electric Transit Buses (NREL/TP-5400-74832). <https://www.nrel.gov/docs/fy20os/ti/74832.pdf>.
- [44] Asian Development Bank. Sustainable Transport Solutions: Low-Carbon Buses in the People's Republic of China. Asian Development Bank, 2018. <https://doi.org/10.22617/TCS189646-2>. (Accessed July 2020).
- [45] Quarles N, Kockelman KM, Mohamed M. Costs and Benefits of Electrifying and Automating Bus Transit Fleets. *Sustainability* 2020;12(10):3977.
- [46] Li Y, Liu K, Foley AM, Zülke A, Berecibar M, Nanini-Maury E, Hostet HE. Data-driven health estimation and lifetime prediction of lithium-ion batteries: A review. *Renew Sustain Energy Rev* 2019;113:109254.
- [47] Dharmakeerthi CH, Mithulanthan N, Saha TK. Impact of electric vehicle fast charging on power system voltage stability. *Int J Electr Power Energy Syst* 2014; 57:241–9.
- [48] Ding H, Hu Z, Song Y. Value of the energy storage system in an electric bus fast charging station. *Appl Energy* 2015;157:630–9.
- [49] Clairand JM, González-Roríquez M, Terán PG, Cedenño I, & Escrivá-Escrivá G. 2020, August. The impact of charging electric buses on the power grid. In 2020 IEEE Power & Energy Society General Meeting (PESGM) (pp. 1–5). IEEE.